(12) INTERNATIONAL APPLICATION PUBLISHED UNDER THE PATENT COOPERATION TREATY (PCT)

(19) World Intellectual Property Organization
International Bureau

(43) International Publication Date
16 September 2021 (16.09.2021)

WIPO | PCT

(10) International Publication Number
WO 2021/181806 A1

(51) International Patent Classification:
H02P 21/13 (2006.01) *H02P 21/22* (2016.01)
H02P 21/18 (2016.01) *H02P 21/32* (2016.01)

(21) International Application Number:
PCT/JP2020/047311

(22) International Filing Date:
11 December 2020 (11.12.2020)

(25) Filing Language: English

(26) Publication Language: English

(30) Priority Data:
20162285.9 11 March 2020 (11.03.2020) EP

(71) Applicant *(for all designated States except JP)*: **MITSUBISHI ELECTRIC CORPORATION** [JP/JP]; 7-3, Marunouchi 2-chome, Chiyoda-ku, Tokyo 1008310 (JP).

(71) Applicant *(for JP only)*: **MITSUBISHI ELECTRIC R&D CENTRE EUROPE B.V.** [NL/NL]; Capronilaan 46, NS Schiphol Rijk1119 (NL).

(72) Inventors: **VOYER, Nicolas**; c/o Mitsubishi Electric R&D Centre Europe, 1 allée de Beaulieu CS 10806, 35708 Rennes Cedex 7 (FR). **BUENO MARIANI, Guilherme**; c/o Mitsubishi Electric R&D Centre Europe, 1 allée de Beaulieu CS 10806, 35708 Rennes Cedex 7 (FR).

(74) Agent: **SOGA, Michiharu**; S. Soga & Co., 2nd Floor, Keihanshin Onarimon Building, 16-12, Shimbashi 6-chome, Minato-ku, Tokyo 1050004 (JP).

(81) Designated States *(unless otherwise indicated, for every kind of national protection available)*: AE, AG, AL, AM, AO, AT, AU, AZ, BA, BB, BG, BH, BN, BR, BW, BY, BZ, CA, CH, CL, CN, CO, CR, CU, CZ, DE, DJ, DK, DM, DO, DZ, EC, EE, EG, ES, FI, GB, GD, GE, GH, GM, GT, HN, HR, HU, ID, IL, IN, IR, IS, IT, JO, JP, KE, KG, KH, KN, KP, KR, KW, KZ, LA, LC, LK, LR, LS, LU, LY, MA, MD, ME, MG, MK, MN, MW, MX, MY, MZ, NA, NG, NI, NO, NZ, OM, PA, PE, PG, PH, PL, PT, QA, RO, RS, RU, RW, SA, SC, SD, SE, SG, SK, SL, ST, SV, SY, TH, TJ, TM, TN, TR, TT, TZ, UA, UG, US, UZ, VC, VN, WS, ZA, ZM, ZW.

(84) Designated States *(unless otherwise indicated, for every kind of regional protection available)*: ARIPO (BW, GH, GM, KE, LR, LS, MW, MZ, NA, RW, SD, SL, ST, SZ, TZ,

(54) Title: METHOD AND DEVICE FOR DETERMINING A POSITION OF A ROTOR OF A THREE-PHASE MOTOR

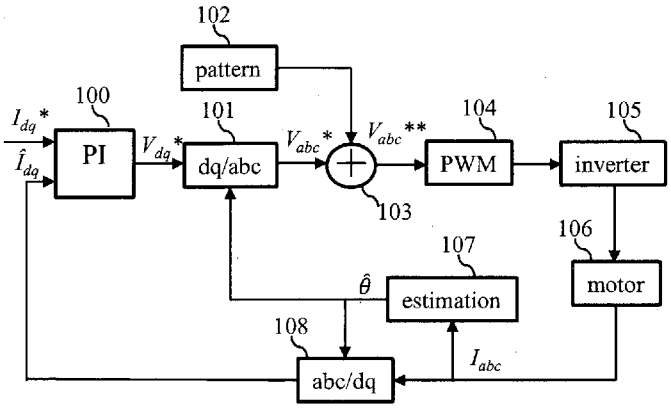


Fig. 1

(57) Abstract: The present invention concerns a method and a device for determining a position of a rotor of a three-phase motor using a FOC system. The invention: - determines, by a proportional-integral controller, a first control voltage vector at a first instant, - transforms the first control voltage vector using an inverse Park transform, - sums the transformed first control voltage vector to a regular polygonal voltage pattern applied during a given duration, - performs a PWM from the sum of the transformed first control voltage vector and the regular polygonal voltage pattern, - controls the motor with the pulse-width modulation, - measures the current at each phase of the motor, -estimates the position of the rotor from the measured currents and from the regular polygonal voltage pattern, - determines, at a second instant, a second control voltage vector from the measured currents and from the estimated position.

[Continued on next page]

WO 2021/181806 A1

UG, ZM, ZW), Eurasian (AM, AZ, BY, KG, KZ, RU, TJ, TM), European (AL, AT, BE, BG, CH, CY, CZ, DE, DK, EE, ES, FI, FR, GB, GR, HR, HU, IE, IS, IT, LT, LU, LV, MC, MK, MT, NL, NO, PL, PT, RO, RS, SE, SI, SK, SM, TR), OAPI (BF, BJ, CF, CG, CI, CM, GA, GN, GQ, GW, KM, ML, MR, NE, SN, TD, TG).

Published:

— *with international search report (Art. 21(3))*

[DESCRIPTION]

[Title of Invention]

METHOD AND DEVICE FOR DETERMINING A POSITION OF A ROTOR OF A THREE-PHASE MOTOR

[Technical Field]

[0001]

The present invention relates generally to a device and a method for determining the position of a rotor of a three-phase motor.

[Background Art]

[0002]

Sensor less control is needed in motor applications for which precise rotor position is needed, and when rotary encoder is not a viable solution, e.g. in low-cost and/or dusty environment. It basically consists in estimating the rotor position by an analysis of electrical waveforms (voltages, currents) available at machine connectors.

[0003]

Some algorithms have been proposed in literature to address this problem. A first class of algorithms are based on observation at a sufficient speed of differences in Back Electromotive Force (BEMF) produced in q and d axes. The BEMF may differ due to presence of permanent magnets and/or due to different inductances in d and q axes (in salient pole machines).

[0004]

At low speeds or standstill, BEMF tends to hide behind the measurement noise floor, other methods must be used such as dI/dt based methods. For salient pole machines, difference in differential inductances enables to estimate the position of the machine from comparison of applied voltage steps and current derivatives. Also for these methods, the measurement noise floor limits the detection ability to cases with sufficient current ripple. At standstill, voltage pulses get very narrow and hard to assert with high precision, e.g. due to switching transients, and current ripple also tends to hide below the measurement noise. High-frequency, high resolution analog-to-digital converters (ADC) are needed for measurements.

[0005]

High frequency voltage injection can be used to produce arbitrary current ripple shapes and increase the signal-to-noise ratio for the estimation. The paper of M. Laumann, C Weiner, and R. Kennel entitled "Arbitrary injection based sensorless control with a defined high frequency current ripple and reduced current and sound level harmonics," published in SLED 2017, discloses a method

that enables the determination of machine position by injecting high frequency voltage for any injected voltage shape. In practice, high frequency injection is producing audible noise, and deserves special care for either rejecting the produced acoustic noise away from audible frequency band or for reducing/spreading the levels of produced harmonics resulting from injection.

[0006]

Most methods rely on availability of inductances or differential inductance values prior to the estimation. This is not so easy to implement in practice with great accuracy, as inductances significantly vary with currents (saturation and/or cross saturation) and temperature profile of the core. Furthermore, the estimation of inductances in the torque producing regions typically requires some specific instrumentation (locked rotor tests, or rotational tests with test load and rotary encoder) to avoid uncontrolled (and potentially dangerous) operation of the machine.

[Summary of Invention]

[0007]

The present invention aims to provide a method and a device for determining a precise rotor position without requiring any inductance value knowledge.

[0008]

To that end, the present invention concerns a method for determining a position of a rotor of a three-phase motor using a field-oriented control system, characterized in that the method comprises the steps of:

- determining, by a proportional-integral controller, a first control voltage vector at a first instant,
- transforming the first control voltage vector using an inverse Park transform,
- summing the transformed first control voltage vector to a regular polygonal voltage pattern, the regular polygonal voltage pattern being applied during a given duration,
- performing a pulse width modulation from the sum of the transformed first control voltage vector and the regular polygonal voltage pattern,
- controlling the motor with the pulse width modulation,
- measuring the current at each phase of the motor,
- estimating the position of the rotor from the measured currents and from the regular polygonal voltage pattern,
- determining, at a second instant, a second control voltage vector from the measured currents and from the estimated position, the time between first and second instants being upper than or equal to the given duration.

The present invention concerns also a device for determining a position of a rotor of a three-phase motor using a field-oriented control system, characterized in that the device comprises:
- means for determining, by a proportional-integral controller, a first control voltage vector at a first instant,
- means for transforming the first control voltage vector using an inverse Park transform,
- means for summing the transformed first control voltage vector to a regular polygonal voltage pattern, the regular polygonal voltage pattern being applied during a given duration,
- means for performing a pulse width modulation from the sum of the transformed first control voltage vector and the regular polygonal voltage pattern,
- means for controlling the motor with the pulse width modulation,
- means for measuring the current at each phase of the motor,
- means for estimating the position of the rotor from the measured currents and from the regular polygonal voltage pattern,
- means for determining, at a second instant, a second control voltage vector from the measured currents and from the estimated position, the time between first and second instants being upper than or equal to the given duration.

[0009]

Thus, the regular polygonal voltage pattern can be used to estimate the rotor position of the motor from the measured currents and in absence of knowledge of motor inductances and saliency. The method can operate under normal operation of the motor, and the variations of first voltage vector do not interfere with the estimation. The method can estimate rotor position in any conditions of the motor (including standstill, low and high speed, and including high torque/current regions).

[0010]

According to a particular feature, the pulse-width modulation is further performed from a carrier signal, the motor is controlled by the pulse-width modulation through an inverter and the currents are measured at the extremums of the carrier signal, the regular polygonal pattern is composed of plural consecutive subperiods, each sub period being equal to an integer number times half the period of the carrier signal, and starting at one extremum of the carrier signal.

[0011]

Thus, the voltage applied to the motor terminals and averaged between successive current measurements precisely matches the sum of the transformed

first control voltage vector and the regular polygonal voltage pattern. The currents measured response of the motor is not affected by crosstalk between voltage vectors composing the regular polygonal voltage pattern.

[0012]

Moreover, as the subperiod duration gets minimised down to half the period of the carrier signal, the minor loops are small, leading to small iron losses and lower audible noise. The pattern duration is also small, so that time between first and second instants is also small: the reactivity of the controller to fast transients is improved.

[0013]

According to a particular feature, the position of the rotor is estimated from a polygonal current response, which is built from a number of current measurements, equal to the number of subperiods plus one, and the difference between the first and last current measurements is used to modify the other current measurements in order to obtain the polygonal current response.

[0014]

Thus, the polygonal current response is closed, and any drift of average current due to presence of ohmic losses and/or back electromotive force caused by rotation is precisely compensated. The modified polygonal current response reflects only HF current variations due to HF voltage injection. As a result, there is no cross-talk between normal operation of the machine and position estimation from the triangular modified current response. The estimation of position is more reliable.

[0015]

According to a particular feature, the regular polygonal pattern is composed of at least three subperiods, the estimation of the position of the rotor from the measured currents and from the regular polygonal voltage pattern is performed using a number of coefficients that is equal to the number of subperiods and the coefficients are determined from the polygonal current response.

[0016]

Thus, the coefficients can easily get determined from the triangular current response. As voltage injection causes the injection of high frequency equilateral flux, one can easily determine the position of the rotor from the observed coefficients.

[0017]

According to a particular feature, the estimation of the position of the rotor from the measured currents and from the regular polygonal voltage pattern is

performed from the polygonal current response that forms a constellation of points using a minimum mean square error method, in order to find a straight line passing through the gravity center of constellation points with an angle and having a minimal distance with the set of points in the constellation, the angle being the position of the rotor.

[0018]

Thus, the estimation of the position can get estimated for any size of regular polygonal voltage pattern. The straight line reflects the direction of highest currents, i.e. the direction with lowest inductance. This inductance can be identified as the rotor axis offering the lowest inductance (typically, the d axis).

[0019]

According to a particular feature, the method comprises further steps of:

- estimating a first rotational speed of the rotor from the first estimated position of the rotor,
- determining the periodicity of the control voltage vector from the first estimated rotational speed,
- determining the periodicity of the regular polygonal voltage pattern from the periodicity of the control voltage vector.

[0020]

Thus, the periodicity of injected regular polygonal voltage pattern is relaxed, reducing the level of noise at low speed. In contrast, at higher speeds, the injection is more frequent, enabling better monitoring of the variations of the rotor position. At high speeds, audible noise caused by injection is masked by other rotational sources of noise.

[0021]

According to a particular feature, the method further comprises the steps of:

- estimating inductance values of the motor from the measured currents and from the regular polygonal voltage pattern,
- determining a value of a voltage that is used to generate the regular polygonal voltage pattern from the estimated inductance values.

[0022]

Thus, the size of voltage pattern is controlled to limit the high frequency response of motor current to a minimum level. When the motor saturates, e.g. in presence of large traction current, smaller voltage injection is needed to get measurable current response. As a result, the size of minor magnetisation loops in the motor is limited, limiting also HF losses and the level of audible noise.

[0023]

According to a particular feature, the method further comprises the step of:
- transforming the second control voltage vector using an inverse Park transform,
- performing a pulse width modulation from the transformed other control voltage vector,
- controlling the motor with the pulse width modulation,
- measuring the current at each phase of the motor,
- estimating a second rotor position of the rotor according to the first estimated rotor position, first estimated rotor speed, and the periodicity of the control voltage vector,
- determining a third control voltage pattern from the measured currents and from the estimated second rotor position.

[0024]

Thus, the control can adjust finely the second voltage vector in absence of injection, in presence of a constant speed. The position and speed is estimated only at occurrence of pattern injection. In absence of injection, the position can be extrapolated. At low speeds, the PI controller can quickly react to sudden torque rise even when the injection pattern is intermittent.

[0025]

According to a particular feature, the regular polygonal voltage pattern has a null average value in a dq reference frame.

[0026]

Thus, the phase-to-phase voltage applied to the motor terminals equals in average that of the first voltage vector. The dynamics of the motor control is not affected by the superposition of the regular voltage pattern. There is no interference between the PI controller and the injection loop used for determining the rotor position. As a result, the sensor less control method is very stable and robust.

[0027]

According to a particular feature, one regular polygonal voltage pattern is summed for each phase and the regular polygonal voltage pattern is inverted or permuted at each determination of a control voltage vector.

[0028]

Thus, the audible noise resulting from successive injection can be randomised. Any undesired non-linear effect in the motor drive gets equally spread over each motor terminal.

[0029]

According to a particular feature, the method further comprises the step of memorizing the estimated inductance values.

[Brief Description of Drawings]

[0030]

The characteristics of the invention will emerge more clearly from a reading of the following description of example embodiments, the said description being produced with reference to the accompanying drawings, among which:

[0031]

[Fig. 1]

Figure 1 represents an example of a Field-Oriented Control system in which the present invention is implemented.

[Fig. 2]

Figure 2 represents an example of PWM signals with a triangular voltage injection according to the invention.

[Fig. 3]

Figure 3 represents the injected voltage pattern.

[Fig. 4]

Figure 4 represents the differential flux response.

[Fig. 5]

Figure 5 represents the differential current response.

[Fig. 6]

Figure 6 represents the constellation of extreme points of current during rotation of the motor.

[Fig. 7]

Figure 7 represents the constellation of extreme points of current during the rotation of the motor after a compensation is applied.

[Fig. 8]

Figure 8 represents an architecture of the estimation module that estimates the position of a rotor of a motor.

[Fig. 9]

Figure 9 represents a first example of an algorithm for estimating the position of a rotor of a motor.

[Fig. 10]

Figure 10 represents measurable geometric relation in a triangular current response.

[Fig. 11]

Figure 11 represents a second example of an algorithm for estimating the position of a rotor of a motor.

[Fig. 12]

Figure 12 represents an identification of q axis by a linear regression method.

[Fig. 13]

Figure 13 represents the distances between constellation points and q axis.

[Fig. 14]

Figure 14 represents an example of an algorithm that may executed by the position evalution module after the execution of the algorithm disclosed in Fig. 9 or 11.

[Fig. 15]

Figure 15 represents the rotational speed of the motor is very low, and the control interval T_{CTRL} between two consecutive voltage patterns is large.

[Fig. 16]

Figure 16 represents the rotational speed of the motor is high, and the estimation module reduces the time interval T_{CTRL}.

[Fig. 17]

Figure 17 represents the rotational speed of the motor is very low, with a large control interval T_{CTRL}.

[Fig. 18]

Figure 18 represents the rotational speed of the motor is very low, with a large control interval T_{CTRL}.

[Description of Embodiments]

[0032]

Fig. 1 represents an example of a Field-Oriented Control system in which the present invention is implemented.

[0033]

Field-Oriented Control (FOC) is a variable-frequency drive control method in which the stator currents of a three-phase AC electric motor are identified as two orthogonal components that can be visualized with a vector. In $\alpha\beta$ reference frame representative of the stator, the vector rotates around the origin in synchronism with the rotor. In dq reference frame representative of the rotor, the vector is stabilised around reference current levels using (PI) controller. Depending on application, current reference can be as example determined from torque reference, which can itself be determined from a speed controller.

[0034]

Typically, proportional-integral (PI) controllers are used to keep the measured current components at their reference values.

[0035]

The Pulse-Width modulation (PWM) of the variable-frequency drive defines the timings of inverter switching according to the stator voltage references that are the output of the PI current controllers.

[0036]

FOC is used to control AC synchronous and induction motors.

[0037]

It was originally developed for high-performance motor applications that are required to operate smoothly over a full speed range, generate full torque at zero speed, and have high dynamic performance including fast acceleration and deceleration.

[0038]

The Field-Oriented Control system comprises a proportional-integral controller PI 100 that calculates the voltages V_d* and V_q* for the torque and flux at the desired speed required by the machine to reach the reference currents I_d* and I_q*. The required voltages V_d* and V_q* are then transformed back to the voltages V_a*, V_b* and V_c* using an inverse Park transform 101. A pattern generation module 102 provides three injection patterns that are respectively added to the voltages V_a*, V_b* and V_c* by an adding module 103. The voltages V_a**, V_b** and V_c** at the output of the adding module 103 are pulse-width modulated by a pulse-width modulation module PWM 104. The pulse-width modulated signals are then provided to inverter legs of a three-phase inverter 105 for regulating an amount of voltage from a DC voltage source not shown in Fig. 1 to be provided to each phase terminals of a motor 106.

[0039]

The current I_a, I_b and I_c are measured at each phase terminal of the motor and provided to an estimation module 107 and to a Park transform module 108. The measurements of I_a, I_b and I_c are performed in a synchronous manner in respect of the PWMs signal. The measurements of I_a, I_b and I_c are performed at points P_1, P_2 and P_3 in Fig. 2. The outputs of the Park transform module 108 $\widehat{I_d}$ and $\widehat{I_q}$ are provided to the proportional-integral controller PI 100. The proportional-integral controller PI 100 compares the measured and reference currents and filters the difference using a weighted sum of proportional and integral terms of the observed difference.

[0040]

It should be noted that the PI controller 100, the transformation modules 101 and 108, the estimation module 107 are activated at a given vector control frequency f_{CTRL}.

[0041]

The estimation module 107 provides an estimate of the angle $\hat{\theta}$ of the rotor to the inverse Park transform 101 and to the Park transform module 108.

[0042]

In Fig. 1, I_{dq}* stands for I_d* and I_q*, V_{dq}* stands for V_d* and V_q*, V_{adc}* stands for V_a*, V_b* and V_c*, V_{adc}** stands for V_a**, V_b** and V_c**, I_{abc} stands for I_c I_a, I_b and I_c and $\widehat{I_{dq}}$ stands for $\widehat{I_d}$ and $\widehat{I_q}$.

[0043]

Fig. 2 represents an example of PWM related signals with a triangular voltage injection according to the invention.

[0044]

As seen in Fig. 2, the injection pattern, named also polygonal regular voltage pattern, is typically composed of 3 PWM subperiods T_1, T_2, T_3 of equal duration $T_c = 1/2f_{sw}$ of a pulse width modulated signal PWMs provided by the pulse-width modulation module PWM 104. The voltages V_a*, V_b* and V_c* issued by the PI controller 100 are assumed constant during the duration of the injection pattern (T_1+T_2+T_3). The voltage pattern varies across subperiods for example as follows. During T_1, the voltage -V_o is added to V_a*, the voltage +V_o is added to V_b* and the voltage +V_o is added to V_c*. During T_2, the voltage +V_o is added to V_a*, the voltage -V_o is added to V_b* and the voltage +V_o is added to V_c*. During T_3, the voltage +V_o is added to V_a*, the voltage +V_o is added to V_b* and the voltage -V_o is added to V_c*. The offset voltage V_o is chosen to provide sufficient current ripple in order to avoid noise and/or interference. The injected HF voltage pattern forms an equilateral triangle in $\alpha\beta$ frame as shown in Figs. 3.

[0045]

It has to be noted here that the regular polygonal voltage patterns are inverted or permuted at each determination of a control voltage vector.

[0046]

According to invention, the injection pattern can be of any size, but is always composed of N subperiods T1, T2, .., TN of equal duration, e.g. Tc = $K/2f_{sw}$, where K is an integer. The sum of voltage pattern across subperiods is identical across each phase, so that the phase-to-phase voltage averaged across the duration of the injection pattern is unmodified by the injection pattern.

[0047]

The PWM controller 104 compares the reference voltage levels V_a**, V_b**, V_c** with the carrier signal PWMs and produces control signals to the inverter 105.

[0048]

The carrier signal PWMs is periodic, with a frequency identical to the switching frequency f_{sw} of inverter legs. The comparison is made at much higher frequency rate (f_{PWM}, few MHz) to keep good controllability of inverter voltage.

[0049]

According to the invention, it should be noted that the switching frequency is not equal to the vector control frequency. Especially, the reference voltage levels V_a*, V_b* and V_c* are constant over the total duration of the injected pattern. Thus, the control frequency is smaller than the switching frequency ($N.f_{CTRL} < 2.f_{sw}$).

[0050]

As example, the carrier signal PWMs is triangular, and the inverter 105 connects in parallel a voltage DC source and one inverter leg per phase. When the reference voltage of one phase gets higher than the carrier signal, the PWM controller 104 switches the corresponding inverter leg into its high state, connecting the phase terminal of the machine to the upper side of the DC voltage source. Reversely, when the reference voltage of one phase gets lower than the carrier signal, the PWM controller switches the corresponding inverter leg into its low state, connecting the phase terminal of the machine to the lower side of the DC voltage source.

[0051]

The addition of a voltage vector to the reference voltages V_a*, V_b*, V_c*, causes the modification of position and duration of inverter states, so as to effectively impose the desired voltage levels, averaged during the period of the carrier signal PWMs.

[0052]

Figs. 3, 4, 5 represent triangular flux injection in a frame.

[0053]

The Fig. 3 represents the injected voltage pattern, the Fig. 4 represents the differential flux response and the Fig. 5 represents the differential current response.

[0054]

The fundamental equation of the system is given as

[0055]

$$V_{abc} = RI_{abc} + \frac{d\phi_{abc}}{dt} \qquad (1)$$

[0056]

In dq frame, this equation becomes

[0057]

$$V_{dq} = RI_{dq} + w\begin{bmatrix}0 & -1\\ 1 & 0\end{bmatrix}\phi_{dq} + \frac{d\phi_{dq}}{dt} \quad (2)$$

[0058]

For salient pole machines, the flux is expressed as

[0059]

$$\phi_{dq} = \begin{bmatrix}L_d & 0\\ 0 & L_q\end{bmatrix} I_{dq} + \phi_{PM} \quad (3)$$

[0060]

In absence of permanent magnets, or assuming that the flux of permanent magnets is constant, $\frac{d\phi_{PM}}{dt} = 0$, we get

[0061]

$$\frac{d\phi_{dq}}{dt} = \begin{bmatrix}L_d & 0\\ 0 & L_q\end{bmatrix}\frac{dI_{dq}}{dt} + \begin{bmatrix}\frac{dL_d}{dt} & 0\\ 0 & \frac{dL_q}{dt}\end{bmatrix} I_{dq} \quad (4)$$

[0062]

from which yields the fundamental relation between HF flux and current terms:

[0063]

$$\frac{d\phi_{dq}}{dt} = \begin{bmatrix}L_d{}' & M_{qd}\\ M_{dq} & L_q{}'\end{bmatrix}\frac{dI_{dq}}{dt} \quad (5)$$

[0064]

where L'_d and L'_q are differential inductances, and M_{qd}, M_{dq} are coupling inductances given by (6) and (7) :

[0065]

$$L'_d = L_d + \frac{dL_d}{dI_d} I_d;\ L'_q = L_q + \frac{dL_q}{dI_q} I_q; \quad (6)$$

[0066]

$$M_{qd} = \frac{dL_d}{dI_q} I_d;\ M_{dq} = \frac{dL_q}{dI_d} I_q \quad (7)$$

[0067]

Using the notation $C = cos(\theta)$, $S = sin(\theta)$, where θ is the direction of the d-axis of the rotor in $\alpha\beta$ frame, the relation becomes (5)

[0068]

$$\frac{d\phi_{\alpha\beta}}{dt} = \begin{bmatrix}C & S\\ -S & C\end{bmatrix}\begin{bmatrix}L_d{}' & M_{qd}\\ M_{dq} & L_q{}'\end{bmatrix}\begin{bmatrix}C & -S\\ S & C\end{bmatrix}\frac{dI_{\alpha\beta}}{dt} \quad (8)$$

[0069]

Eventually, (8) rewrites as (9), which is the fundamental relation linking variations of current with variations of flux in $\alpha\beta$ frame.

[0070]

$$\frac{dI_{\alpha\beta}}{dt} = \begin{bmatrix} B-\Delta & A+X_2 \\ A+X_1 & D+\Delta \end{bmatrix} \frac{d\phi_{\alpha\beta}}{dt} \qquad (9)$$

[0071]

where A, B, D, X_1, X_2 have the following expressions :

[0072]

$$A = CS\left(\frac{1}{L_{d'}} - \frac{1}{L_{q'}}\right), B = \frac{C^2}{L_{d'}} + \frac{S^2}{L_{q'}}, D = \frac{S^2}{L_{d'}} + \frac{C^2}{L_{q'}}, \qquad (10)$$

[0073]

$$X_1 = \frac{S^2 M_{qd} - C^2 M_{dq}}{L_{d'}L_{q'} - M_{qd}M_{dq}}, X_2 = \frac{S^2 M_{dq} - C^2 M_{qd}}{L_{d'}L_{q'} - M_{qd}M_{dq}},$$

$$\Delta = -CS\frac{M_{qd}+M_{dq}}{L_{d'}L_{q'} - M_{qd}M_{dq}} \qquad (11)$$

[0074]

From (10), a direct resolution of unknowns θ, $L_d{}'$, $L_q{}'$ can be reached upon observation of parameters A, B, D :

[0075]

$$tan(2\theta) = \frac{2A}{B-D} \qquad (12)$$

[0076]

$$L_d{}' = \frac{2}{D+B+\frac{2A}{sin(2\hat{\theta})}} \qquad (13)$$

[0077]

$$L_q{}' = \frac{2}{D+B-\frac{2A}{sin(2\hat{\theta})}} \qquad (14)$$

[0078]

The problem of direct estimation of position and of differential inductances therefore consists in identifying the parameters A, B, D from the observed triangular current response.

[0079]

At standstill, when the machine has zero speed, zero acceleration, the reference voltage V_a*, V_b*, V_c* from PI controller 100 precisely compensates for the ohmic losses. The flux evolves in $\alpha\beta$ frame between 3 flux points $\phi_{\alpha\beta_1}$, $\phi_{\alpha\beta_2}$, $\phi_{\alpha\beta_3}$, as shown in Fig. 4, which can be determined by time integration of the injected voltage pattern.

[0080]

$$\begin{cases} \overrightarrow{\phi_{\alpha\beta_1}} = \overrightarrow{\phi_G} + \frac{V_o T_c}{\sqrt{3}} \begin{bmatrix} \sqrt{3} \\ 1 \end{bmatrix} \\ \overrightarrow{\phi_{\alpha\beta_2}} = \overrightarrow{\phi_G} + \frac{V_o T_c}{\sqrt{3}} \begin{bmatrix} -\sqrt{3} \\ 1 \end{bmatrix} \\ \overrightarrow{\phi_{\alpha\beta_3}} = \overrightarrow{\phi_G} + \frac{V_o T_c}{\sqrt{3}} \begin{bmatrix} 0 \\ -2 \end{bmatrix} \end{cases} \quad (15)$$

[0081]

where $\overrightarrow{\phi_G} = (\overrightarrow{\phi_{\alpha\beta_1}} + \overrightarrow{\phi_{\alpha\beta_2}} + \overrightarrow{\phi_{\alpha\beta_3}})/3$ is the gravity point of the constellation of flux points. Because of the structure of applied voltage pattern (rotation of 120° and equal duration of subperiods) , extreme flux points together form an equilateral triangle in $\alpha\beta$ reference frame.

[0082]

From (9), we derive that currents necessarily evolve in $\alpha\beta$ frame between 3 current points $I_{\alpha\beta_1}$, $I_{\alpha\beta_2}$, $I_{\alpha\beta_3}$ as shown in Fig. 5.

[0083]

$$\begin{cases} \overrightarrow{I_{\alpha\beta_1}} = \overrightarrow{I_G} + \frac{V_o T_c}{\sqrt{3}} \begin{bmatrix} (B-\Delta)\sqrt{3} + A + X_2 \\ \sqrt{3}(A + X_1) + D + \Delta \end{bmatrix} \\ \overrightarrow{I_{\alpha\beta_2}} = \overrightarrow{I_G} + \frac{V_o T_c}{\sqrt{3}} \begin{bmatrix} -(B-\Delta)\sqrt{3} + A + X_2 \\ -\sqrt{3}(A + X_1) + D + \Delta \end{bmatrix} \\ \overrightarrow{I_{\alpha\beta_3}} = \overrightarrow{I_G} + \frac{V_o T_c}{\sqrt{3}} \begin{bmatrix} -2(A + X_2) \\ -2(D + \Delta) \end{bmatrix} \end{cases} \quad (16)$$

[0084]

where $\overrightarrow{I_G} = (\overrightarrow{I_{\alpha\beta_1}} + \overrightarrow{I_{\alpha\beta_2}} + \overrightarrow{I_{\alpha\beta_3}})/3$ is the gravity point of the constellation of extreme current points.

[0085]

Assuming current sampling at the edges or extemums of PWMs signal carrier i.e. at points P_1, P_2 and P_3 of Fig. 2, the current measurements are operated away from switching events and are not affected by associated ringing. At these sampling times, all motor legs are always connected to the same side of DC bus, and measured currents can be regarded as positioned at extreme points $I_{\alpha\beta_1}$, $I_{\alpha\beta_2}$, $I_{\alpha\beta_3}$.

[0086]

The invention also applies when durations of subperiods are equal to an integer number K of half switching cycles, with a sampling frequency further reduced to $2f_{sw}/K$, and sampling timings still located at the edges of PWM signal carrier.

[0087]

Irrespective of inductance levels, the triangle formed by extreme points $I_{\alpha\beta_1}$, $I_{\alpha\beta_2}$, $I_{\alpha\beta_3}$ is naturally elongated in the direction of the q axis for machines exhibiting some saliency ratio $\frac{L_d}{L_q} > 1$.

[0088]

Under rotation, the PI controller 100 outputs a voltage reference that compensates for ohmic losses and for the back electromotive force (BEMF) of the motor 106 causing the average flux to turn in $\alpha\beta$ frame synchronously with the rotor with a given speed, which can be assumed constant over the duration of the injection pattern. The added voltage pattern produces HF variations of flux, superposed to the average rotating flux, and the HF variations of flux keep following equation (15) yet with a gravity center sliding with time.

[0089]

From equation (9), we can see that the current response will follow the same behavior: HF variations according to equation (16), with a gravity center also sliding in time. This causes the constellation of points of current to no longer follow a regular structure, as it will be disclosed in Figs. 6, 7.

[0090]

Fig. 6 represents the constellation of extreme points of current during rotation of the motor.

[0091]

Fig. 7 represents the constellation of extreme points of current during the rotation of the motor after a compensation is applied.

[0092]

Once having completed a full triangular turn, the current $I_{\alpha\beta_4}$ measured at the end of injection is no longer aligned with the current $I_{\alpha\beta_1}$ measured just before the injection of triangular pattern, due to the rotational condition.

[0093]

Equations (16) with constant (not gliding) gravity point can be maintained when applied to modified current levels $I_{\alpha\beta_1}{}'$, $I_{\alpha\beta_2}{}'$, $I_{\alpha\beta_3}{}'$ which are postprocessed according to (17) to compensate for the misalignment between measured currents $I_{\alpha\beta_1}$ and $I_{\alpha\beta_4}$ over one injection pattern cycle :

[0094]

$$\begin{cases} \overrightarrow{I_{\alpha\beta_1}{}'} = \overrightarrow{I_{\alpha\beta_4}} \\ \overrightarrow{I_{\alpha\beta_2}{}'} = \overrightarrow{I_{\alpha\beta_2}} + 2\left(\overrightarrow{I_{\alpha\beta_4}} - \overrightarrow{I_{\alpha\beta_1}}\right)/3 \\ \overrightarrow{I_{\alpha\beta_3}{}'} = \overrightarrow{I_{\alpha\beta_3}} + \left(\overrightarrow{I_{\alpha\beta_4}} - \overrightarrow{I_{\alpha\beta_1}}\right)/3 \end{cases} \qquad (17)$$

[0095]

It should be noted that the modification of current levels which suppresses the gliding of gravity center can equally be applied to non triangular patterns, i.e. any polygonal regular patterns.

[0096]

Fig. 8 represents an architecture of the estimation module that estimates the position of a rotor of a motor.

[0097]

The estimation module 107 has, for example, an architecture based on components connected together by a bus 501 and a processor 500 controlled by a program.

[0098]

The bus 501 links the processor 500 to a read only memory ROM 502, a random access memory RAM 503, and an input output I/O interface I/F 505.

[0099]

The input output interface I/F 505 receives the currents measurements Ia, Ib and Ic and provides the angle $\hat{\theta}$ of the rotor to the inverse Park transform 101 and to the Park transform module 108.

[0100]

The memory 503 contains registers intended to receive variables and the instructions of the program related to the algorithm disclosed in Fig. 6 or 8 or 10.

[0101]

The read-only memory, or possibly a flash memory 502, contains instructions of the program related to the algorithm disclosed in Fig. 6 or 8 or 10.

[0102]

When the estimation module 107 is powered on, the instructions stored in the memory 503 are transferred to the random access memory 503.

[0103]

The estimation module 107 may be implemented in software by execution of a set of instructions or program by a programmable computing machine, such as a PC (*Personal Computer*), a DSP (*Digital Signal Processor*) or a microcontroller; or else implemented in hardware by a machine or a dedicated component, such as an FPGA (*Field-Programmable Gate Array*) or an ASIC (*Application-Specific Integrated Circuit*).

[0104]

In other words, the estimation module 107 includes circuitry enabling the estimation module 107 to perform the program.

[0105]

Fig. 9 represents a first example of an algorithm for estimating the position of a rotor of a motor.

[0106]

Neglecting the effect of coupling inductances M_{qd}, $M_{dq} \cong 0$, the fundamental equation (9) becomes

$$\frac{dI_{\alpha\beta}}{dt} = \begin{bmatrix} B & A \\ A & D \end{bmatrix} \frac{d\phi_{\alpha\beta}}{dt} \qquad (18)$$

As seen in Fig. 7, A, B, D parameters are then related to measured current vectors by (19).

[0107]

$$\begin{cases} \overrightarrow{I_{\alpha\beta_1}} = \overrightarrow{I_G} + \frac{V_o T_c}{\sqrt{3}} \begin{bmatrix} \mathrm{B}\sqrt{3} + A \\ \sqrt{3}\mathrm{A} + D \end{bmatrix} \\ \overrightarrow{I_{\alpha\beta_2}} = \overrightarrow{I_G} + \frac{V_o T_c}{\sqrt{3}} \begin{bmatrix} -\mathrm{B}\sqrt{3} + A \\ -\sqrt{3}\mathrm{A} + D \end{bmatrix} \\ \overrightarrow{I_{\alpha\beta_3}} = \overrightarrow{I_G} + \frac{V_o T_c}{\sqrt{3}} \begin{bmatrix} -2\mathrm{A} \\ -2\mathrm{D} \end{bmatrix} \end{cases} \qquad (19)$$

[0108]

Fig. 10 represents measurable geometric relation in a triangular current response.

[0109]

More precisely, the geometrical relations are shown by omitting a scale factor of $\frac{V_o T_c}{\sqrt{3}}$.

[0110]

In absence of noise, we observe that A can be obtained by two independent calculation paths :

[0111]

$$A = \frac{I_{\beta_1} - I_{\beta_2}}{4V_o T} = \frac{\left(I_{\alpha_G} - I_{\alpha_3}\right)\sqrt{3}}{4V_o T} \qquad (20)$$

[0112]

At step S61, the estimation module 107 determines A using the formula noted 20.

[0113]

At step S62, the estimation module 107 determines B and D using the following equation system :

[0114]

$$\begin{cases} A = \frac{I_{\beta_1} - I_{\beta_2} + \left(I_{\alpha_G} - I_{\alpha_3}\right)\sqrt{3}}{4V_o T_c} \\ B = \frac{I_{\alpha_1} - I_{\alpha_2}}{2V_o T_c} \\ D = \frac{\left(I_{\beta_G} - I_{\beta_3}\right)\sqrt{3}}{2V_o T_c} \end{cases} \quad (21)$$

[0115]

Thus, upon observation of triangular current response and neglecting effect of coupling inductances, the estimation module 107 can derive coefficients (A, B, D) from (19), and ultimately determine at step S63 position θ and differential inductances using the following formulas :

[0116]

$$tan(2\theta) = \frac{2A}{B-D} \quad (12)$$

$$L_d{}' = \frac{2}{D+B+\frac{2A}{sin(2\hat{\theta})}}$$

$$L_q{}' = \frac{2}{D+B-\frac{2A}{sin(2\hat{\theta})}}$$

[0117]

The estimated inductance values may be memorized for example in a look up table.

[0118]

Fig. 11 represents a second example of an algorithm for estimating the position of a rotor of a motor.

[0119]

The effect of saliency typically causes the current to respond to a circular flux excitation with an elliptic shape. In absence of coupling inductances, the large axis of the elliptic shape can be considered aligned with q axis.

[0120]

A linear regression may be applied for the direct detection of q axis from measured current response to injected equilateral flux.

[0121]

At step S81, the estimation module 107 applies a Minimum Means Square Error method.

[0122]

In a particular example, the injection patterns is triangular. Let us consider the constellation of three summits (x_k, y_k) of current response, expressed relatively to the gravity center of that constellation.

[0123]

$$\begin{cases} x_k = I_{k\alpha} - I_{G\alpha} \\ y_k = I_{k\beta} - I_{G\beta} \end{cases} \quad (31)$$

[0124]

As seen in Figs. 12-13, the Minimum Mean Square Error (MMSE) method consists in finding the straight line passing through the gravity center with an angle θ with ox axis, the straight line having a minimal distance D with the set of points in the constellation.

[0125]

Fig. 12 represents an identification of q axis by a linear regression method and Fig. 13 represents the distances between constellation points and q axis.

[0126]

If constellation points are projected on the straight line perpendicularly to that line, the projected points (x_{pk}, y_{pk}) must verify the equation system :

[0127]

$$\begin{cases} (x_k - x_{pk}).+(y_k - y_{pk}).a = 0 \\ ax_{pk} = y_{pk} \end{cases} \quad (32)$$

[0128]

where $a = tan(\theta_q)$. This system solves as

[0129]

$$\begin{cases} x_{pk} = \frac{x_k + ay_k}{1+a^2} \\ y_{pk} = \frac{ax_k + a^2 y_k}{1+a^2} \end{cases} \quad (33)$$

[0130]

The square distance of a constellation point to the straight line is then given as :

[0131]

$$d^2(k,\theta) = (x_k - x_{pk})^2 + (y_k - y_{pk})^2 = \frac{(y_k - ax_k)^2}{1+a^2} \quad (34)$$

[0132]

The minimum total square distance of straight line to the constellation points must verify:

[0133]

$$\frac{dD^2 = \sum_k {d_k}^2}{da} = 0 \Leftrightarrow \frac{d}{da}\sum_k \frac{(y_k - ax_k)^2}{1+a^2} = 0 \quad (35)$$

[0134]

leading to a second order polynomial of term a.

[0135]

$$a^2 \sum_k x_k y_k + a(\sum_k {x_k}^2 - \sum_k {y_k}^2) - \sum_k x_k y_k = 0 \quad (36)$$

[0136]

The solution is then given as:

[0137]

$$a = tan(\theta_q) = \frac{-\chi \pm \sqrt{\chi^2+4}}{2} \qquad (37)$$

[0138]

where $$\chi = \frac{\sum_k x_k{}^2 - \sum_k y_k{}^2}{\sum_k x_k y_k} \qquad (38)$$

[0139]

Both solutions correspond to straight lines with minimum (q axis) and maximum distances to the constellation points. For positive sign of $\sum_k x_k y_k$, the derivative of the distance is first positive, negative, then positive, so that only the highest optimum is a local minimum. The solution choice is alternated for negative sign of $\sum_k x_k y_k$.

[0140]

$$\begin{cases} \sum_k x_k y_k > 0 \Rightarrow \theta_q = atan\left(\frac{-\chi+\sqrt{\chi^2+4}}{2}\right) \\ \sum_k x_k y_k < 0 \Rightarrow \theta_q = atan\left(\frac{-\chi-\sqrt{\chi^2+4}}{2}\right) \\ \sum_k x_k y_k = 0, \begin{cases} \sum_k x_k{}^2 > \sum_k y_k{}^2 \Rightarrow \theta_q = 0 \\ \sum_k x_k{}^2 < \sum_k y_k{}^2 \Rightarrow \theta_q = \pi/2 \end{cases} \end{cases} \qquad (39)$$

[0141]

Thus, using equations (38) and (39), we can determine the angle θ_q of the q axis.

[0142]

At step S82, the estimation module 107 determines the rotor angle as:

[0143]

$$\theta = \theta_q - \pi/2 \qquad (40)$$

[0144]

Differential inductances can also get estimated from the distance DI_q, DI_d of current constellation point to the optimal straight lines.

[0145]

$$\begin{cases} DI_q = \sqrt{\frac{\sum_k y_k{}^2 - 2\sum_k x_k y_k a + \sum_k x_k{}^2 a^2}{1+a^2}} \\ DI_d = \sqrt{\frac{\sum_k y_k{}^2 + 2\sum_k x_k y_k / a + \sum_k x_k{}^2 / a^2}{1+1/a^2}} \end{cases} \qquad (41)$$

[0146]

For equilateral flux triangles formulated by equation (15), the distance of flux constellation points to any straight line can be reduced to a constant, whatever the director coefficient b of the straight line:

[0147]

$$D\phi_b = \frac{V_o T_c}{\sqrt{3}} \sqrt{\frac{\left(1+b\sqrt{3}\right)^2+\left(1-b\sqrt{3}\right)^2+(-2)^2}{1+b^2}} = V_o T_c \sqrt{2} \quad (42)$$

[0148]

At step S83, the estimation module 107 determines inductances estimated as:

[0149]

$$\begin{cases} L'_d = \frac{D\phi_d}{DI_d} \\ L'_q = \frac{D\phi_q}{DI_q} \end{cases} \quad (43)$$

[0150]

It should be noted that formulas (32) to (41) are equally applicable for non- triangular constellations, i.e. for polygonal/circular voltage injection patterns.

[0151]

The estimated inductance values may be memorized for example in a look up table.

[0152]

Fig. 14 represents an example of an algorithm that may executed by the position evalution module after the execution of the algorithm disclosed in Fig. 9 or 11.

[0153]

At step S10, the estimation module 107 estimates the rotational speed of the rotor from estimated position. The estimation module 107 estimates the rotational speed as $\omega_e = \frac{d\theta}{dt}$.

[0154]

At step S11, the estimation module 107 determines the vector control frequency f_{CTRL} from the estimated speed. The vector control frequency is the frequency at which operates the proportional-integral controller PI 100, the inverse Park transform 101, the estimation module 107 and the Park transform module 108. For example, the estimation module 107 determines the vector control frequency as $f_{CTRL} = \frac{\omega_e}{2\pi} \frac{180}{\Delta\theta}$, $\Delta\theta$ is the position error resulting of the system latency in presence of speed. At that step, the estimation module 107

determines the control interval T_{CTRL} as the inverse of the vector control frequency f_{CTRL}.

[0155]

At step S12, the estimation module 107 determines the injection pattern frequency from the estimated speed. For example, the estimation module 107 determines the injection pattern frequency as $f_{inject} = f_{CTRL}/P$ where P is the ratio between vector control frequency f_{CTRL} and an unaudible low frequency, e.g. 100Hz.

[0156]

At low speeds, this enables to reduce the injection frequency, and thus reduces audible noise generated by the injected pattern. In addition, HF iron losses are reduced. The accuracy of position in presence of speed is constant.

[0157]

At step S13, the estimation module 107 determines an injection voltage level V_o from the estimated inductances and an injection frequency f_{inject}.

[0158]

This enables to keep current variations resulting from HF injection to some stabilised level, regardless of saturation conditions, and change of injection frequency. The current variations can be optimised to fight for measurement noise floor, while minimising HF iron losses.

[0159]

As example, $V_o = L.\Delta I f_{inject}$, where ΔI is a target level of current variations due to injection and L is an inductance estimated at step S63 or step S83. As example, L is the smallest inductance among L_d' and L_q'.

[0160]

At next step S14, the estimation module 107 determines the duration of subperiods of injection pattern. The duration of subperiods is a multiple K of half switching periods ($1/2f_{sw}$). For example, the estimation module 107 determines $K = 2f_{sw}/Nf_{inject}$, where N is the size of polygonal voltage pattern, for example three in the example of Fig. 2.

[0161]

Figs. 15-18 represent in plain line the time variations of the reference voltage V_a** of one phase according to various embodiments of the invention.

[0162]

Only one phase is represented for the sake of clarity, but the embodiments equally apply to the other phases.

[0163]

In each Fig. 11a, 11b, 11c, 11d, the voltage pattern has duration $T_{pattern}$, which is the sum of subperiods, and a size equal to the offset voltage V_o. The duration of voltage pattern is always smaller than the control interval T_{CTRL}, the time interval between consecutive updates of control voltage vector according to the invention, and the voltage pattern is superposed to the control voltage vector V_a*, which is represented in dashed line.

[0164]

In Fig. 15, the rotational speed of the motor is very low, and the control interval T_{CTRL} between two consecutive voltage patterns is large. The number of minor flux loops resulting from the invention is small, resulting in limited iron losses in the magnetic core of the machine.

[0165]

In Fig. 16, the rotational speed of the motor is high, and the estimation module 107 reduces at step S11 the time interval T_{CTRL}. The controllability of the motor is increased compared with Fig. 15, the rotor position can be determined at high speed.

[0166]

In Fig. 17, the rotational speed of the motor is very low, with a large control interval T_{CTRL}, identical to the one in Fig. 15. The estimation module 107 increases the duration of voltage pattern according to step S12, and also reduces the offset voltage V_o. The number and size of minor flux loops is identical to the one of Fig. 15.

[0167]

Compared with Fig 15, the injection frequency is smaller. As a result, the audible noise generated by the voltage pattern is shifted to low frequencies, and produces less burden to human ears. Furthermore, the current response is less prone to high frequency effects (e.g. eddy currents, excess loss), and level of HF iron losses resulting from voltage injection is reduced.

[0168]

In Fig. 18, the rotational speed of the motor is very low, with a large control interval T_{CTRL}, identical to that in Fig. 15. In this example, the voltage pattern is injected only once every $K=3$ control intervals. At control intervals including injection, the estimation module 107 estimates rotor position as in step S63, and also estimates the speed of the motor from estimated rotor position. At control intervals without injection, the estimation module 107 extrapolates the rotor position according to last estimated rotor position, last estimated rotor speed, and T_{CTRL} determined at step S11. Estimation module 107 serialises the estimated and

extrapolated position towards modules 101 and 108, so that current controller keeps fast operation in spite of absence of injection patterns.

[0169]

As example, the rotor position *Theta* at time *t* is extrapolated from last known rotor position and rotor speed at time t_{last} from $Theta(t) = Theta(t_{last}) + Speed*(t-t_{last})$. The speed is estimated at control intervals including injection as $Speed = (Theta(t_{inj,n})-Theta(t_{inj,n-1}))/(t_{inj,n}-t_{inj,n-1})$, where $Theta(t_{inj,n})$ is the rotor position estimated according to the invention at steps S63 or S82.

[CLAIMS]

[Claim 1]

A method for determining a position of a rotor of a three-phase motor using a field oriented control system, characterized in that the method comprises the steps of:

- determining, by a proportional-integral controller, a first control voltage vector at a first instant,
- transforming the first control voltage vector using an inverse Park transform,
- summing the transformed first control voltage vector to a regular polygonal voltage pattern, the regular polygonal voltage pattern being applied during a given duration,
- performing a pulse-width modulation from the sum of the transformed first control voltage vector and the regular polygonal voltage pattern,
- controlling the motor with the pulse-width modulation,
- measuring the current at each phase of the motor,
- estimating the position of the rotor from the measured currents and from the regular polygonal voltage pattern,
- determining, at a second instant, a second control voltage vector from the measured currents and from the estimated position, the time between first and second instants being upper than or equal to the given duration.

[Claim 2]

The method according to claim 1, characterized in that the pulse-width modulation is further performed from a carrier signal, the motor is controlled by the pulse-width modulation through an inverter and the currents are measured at the extremums of the carrier signal, the regular polygonal pattern being composed of plural consecutive subperiods, each subperiod being equal to an integer number times half the period of the carrier signal, and starting at one extremum of the carrier signal.

[Claim 3]

The method according to claim 2, characterized in that the position of the rotor is estimated from a polygonal current response, which is built from a number of current measurements, equal to the number of subperiods plus one, and the difference between the first and last current measurements is used to modify the other current measurement in order to obtain the polygonal current response.

[Claim 4]

The method according to claim 3, characterized in that the regular polygonal pattern is composed of at least three subperiods, the estimation of the

position of the rotor from the measured currents and from the regular polygonal voltage pattern is performed using a number of coefficients that is equal to the number of subperiods and the coefficients are determined from the polygonal current response.

[Claim 5]

The method according to claim 3, characterized in that the estimation of the position of the rotor from the measured currents and from the regular polygonal voltage pattern is performed from the polygonal current response that forms a constellation of points using a minimum mean square error method, in order to find a straight line passing through the gravity center of constellation of points with an angle and having a minimal distance with the set of points in the constellation, the angle being the position of the rotor.

[Claim 6]

The method according to any of the claims 3 to 5, characterized in that the method comprises further steps of:

- estimating a first rotational speed of the rotor from the first estimated position of the rotor,
- determining the periodicity of the control voltage vector from the first estimated rotational speed,
- determining the periodicity of the regular polygonal voltage pattern from the periodicity of the control voltage vector.

[Claim 7]

The method according to claims 3 to 6, characterized in that the method further comprises the steps of:

-estimating inductance values of the motor from the measured currents and from the regular polygonal voltage pattern,
- determining a value of a voltage that is used to generate the regular polygonal voltage pattern from the estimated inductance values.

[Claim 8]

The method according to claim 6, characterized in that the method further comprises the step of:

- transforming the second control voltage vector using an inverse Park transform,
- performing a pulse-width modulation from the transformed second control voltage vector,
- controlling the motor with the pulse-width modulation,
- measuring the current at each phase of the motor,

- estimating a second rotor position of the rotor according to the first estimated rotor position, first estimated rotor speed, and the periodicity of the control voltage vector,

- determining a third control voltage pattern from the measured currents and from the estimated second rotor position.

[Claim 9]

The method according to claim 1 or 2, characterized in that the regular polygonal voltage pattern has a null average value in a dq reference frame.

[Claim 10]

The method according to claim 9, characterized in that one regular polygonal voltage pattern is summed for each phase and the regular polygonal voltage pattern is inverted or permuted at each determination of a control voltage vector.

[Claim 11]

The method according to claim 6, characterized in that the method further comprises the step of memorizing the estimated inductance values.

[Claim 12]

A device for determining a position of a rotor of a three-phase motor using a field-oriented control system, characterized in that the device comprises:

- means for determining, by a proportional-integral controller, a first control voltage vector at a first instant,

- means for transforming the first control voltage vector using an inverse Park transform,

- means for summing the transformed first control voltage vector to a regular polygonal voltage pattern, the regular polygonal voltage pattern being applied during a given duration,

- means for performing a pulse-width modulation from the sum of the transformed first control voltage vector and the regular polygonal voltage pattern,

- means for controlling the motor with the pulse-width modulation,

- means for measuring the current at each phase of the motor,

- means for estimating the position of the rotor from the measured currents and from the regular polygonal voltage pattern,

- means for determining, at a second instant, a second control voltage vector from the measured currents and from the estimated position, the time between first and second instants being upper than or equal to the given duration.

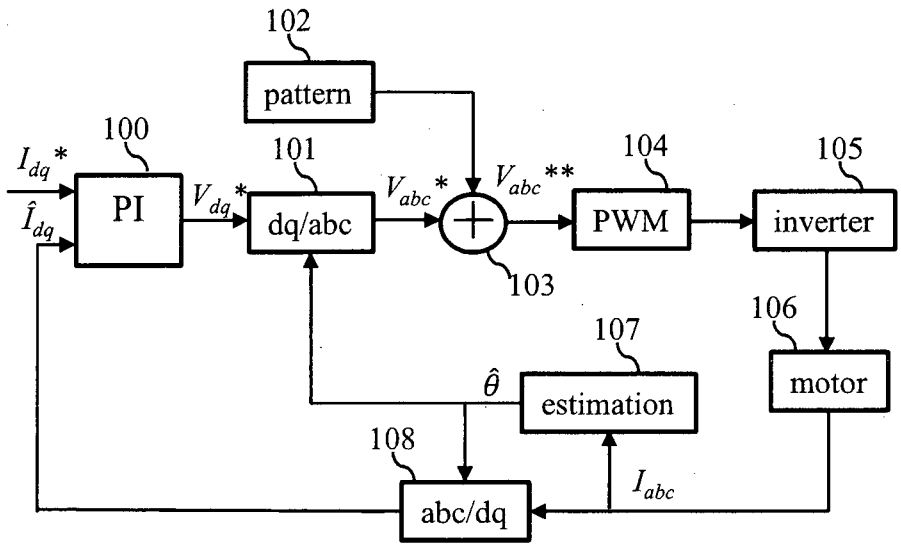

102
pattern
100
101
104
105
I_{dq}*
$\hat{I}_{dq}$
PI
V_{dq}*
dq/abc
V_{abc}*
V_{abc}**
PWM
inverter
103
106
107
motor
$\hat{\theta}$
estimation
108
I_{abc}
abc/dq

Fig. 1

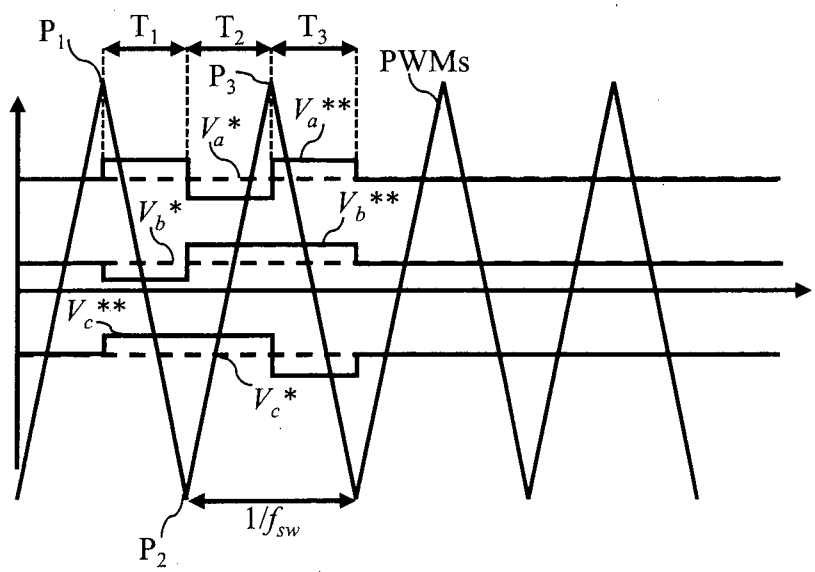

P1
T1
T2
T3
PWMs
P3
V_a*
V_a**
V_b*
V_b**
V_c**
V_c*
1/f_{sw}
P2

Fig. 2

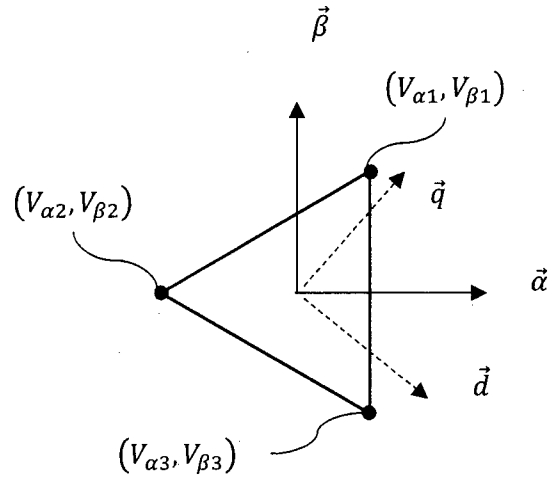


Fig. 3

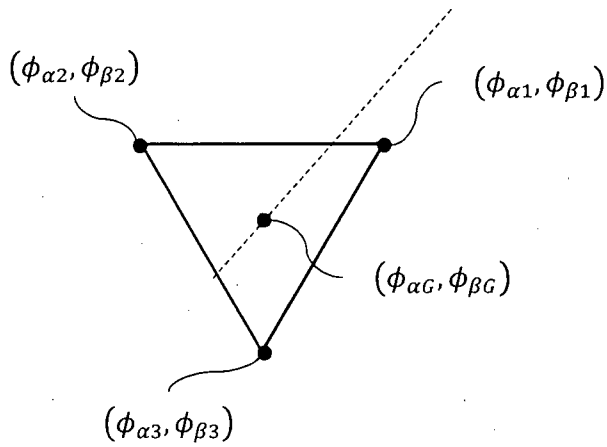


Fig. 4

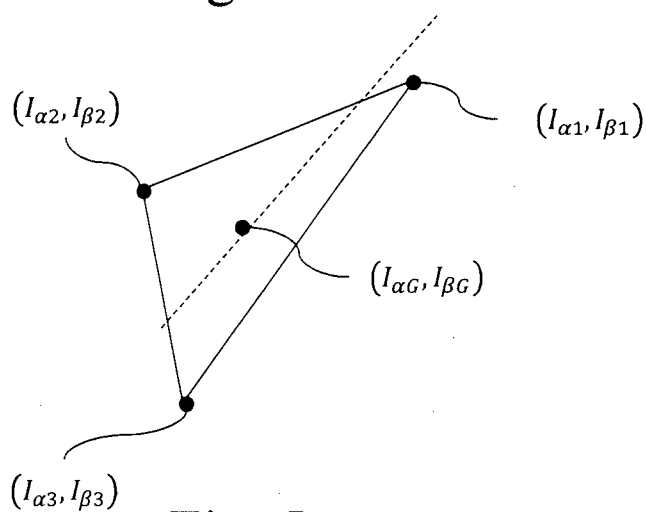


Fig. 5

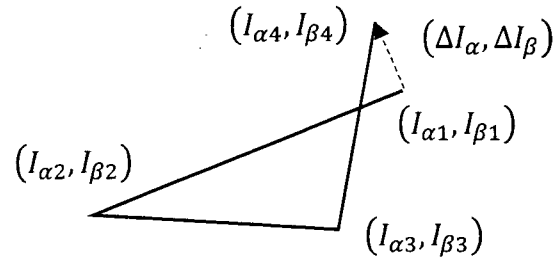


Fig. 6

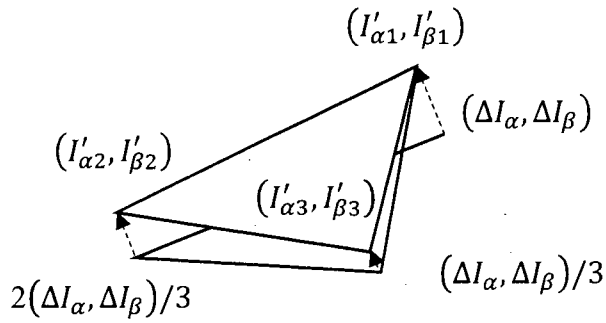


Fig. 7

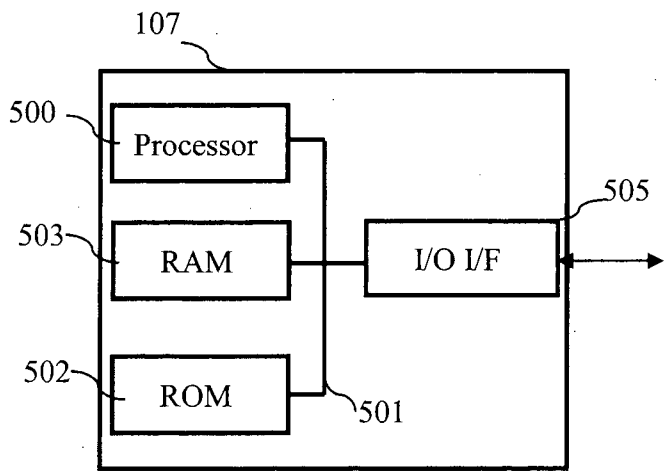


Fig. 8

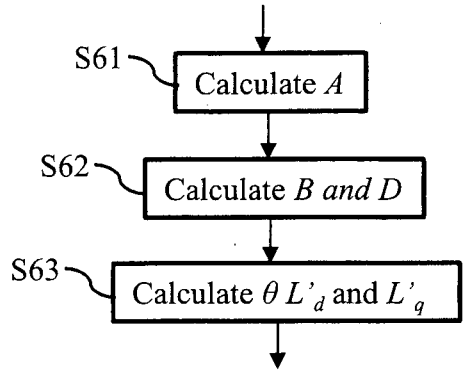

S61
Calculate A
S62
Calculate B and D
S63
Calculate θ L'd and L'q

Fig. 9

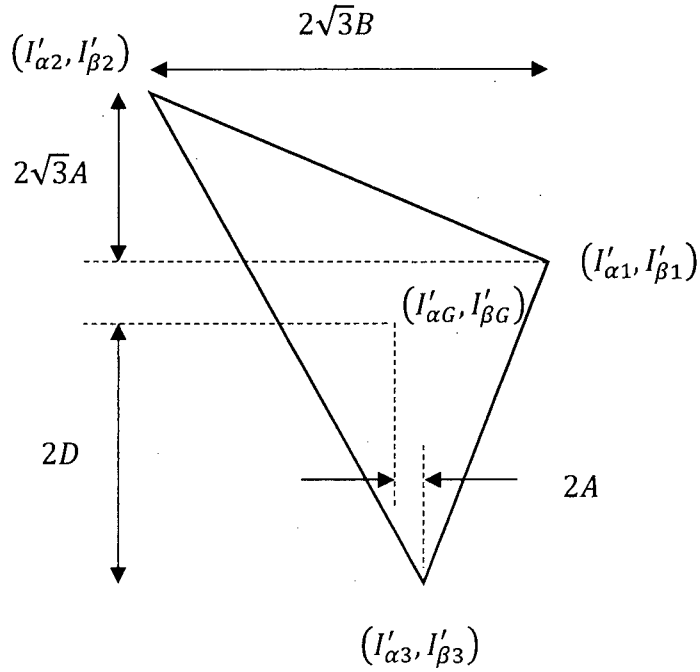

$2\sqrt{3}B$
$(I'_{\alpha 2}, I'_{\beta 2})$
$2\sqrt{3}A$
$(I'_{\alpha 1}, I'_{\beta 1})$
$(I'_{\alpha G}, I'_{\beta G})$
$2D$
$2A$
$(I'_{\alpha 3}, I'_{\beta 3})$

Fig. 10

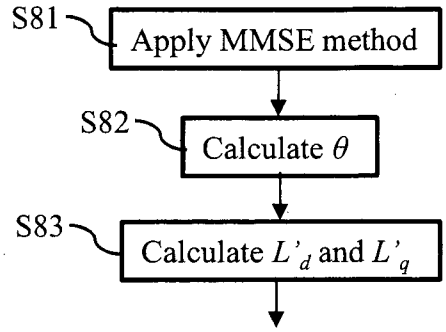


Fig. 11

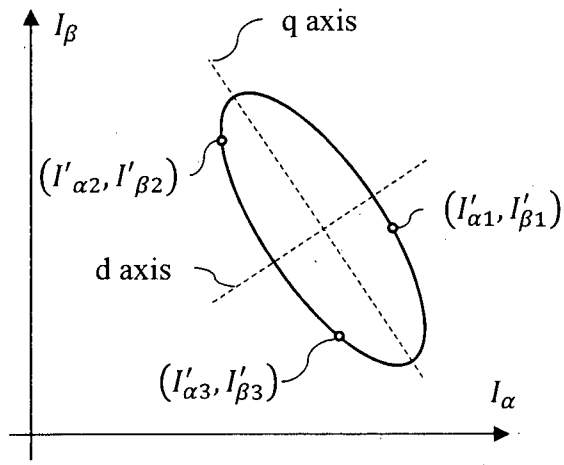


Fig. 12

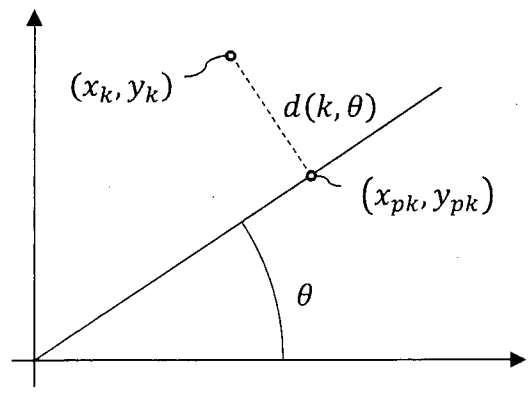


Fig. 13

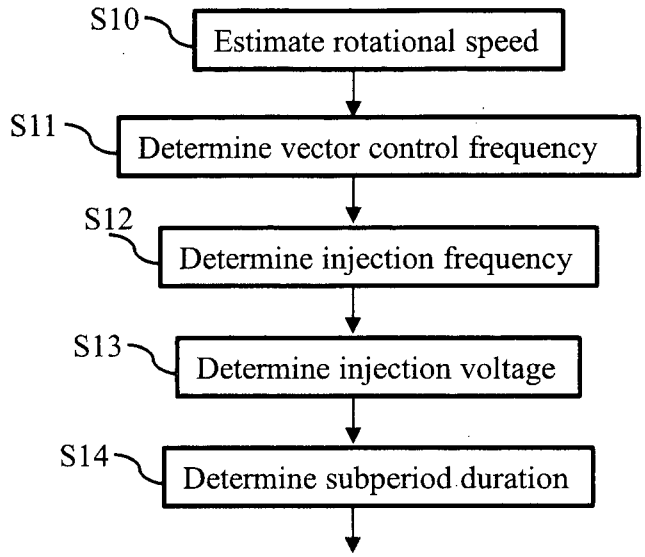

S10
Estimate rotational speed
S11
Determine vector control frequency
S12
Determine injection frequency
S13
Determine injection voltage
S14
Determine subperiod duration

Fig. 14

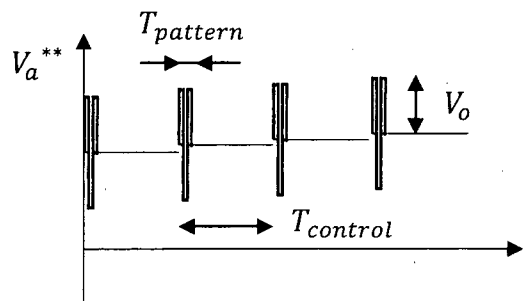

$T_{pattern}$
V_a^{**}
V_o
$T_{control}$

Fig. 15

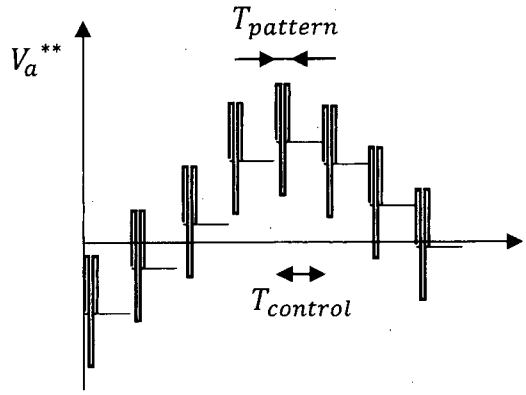


Fig. 16

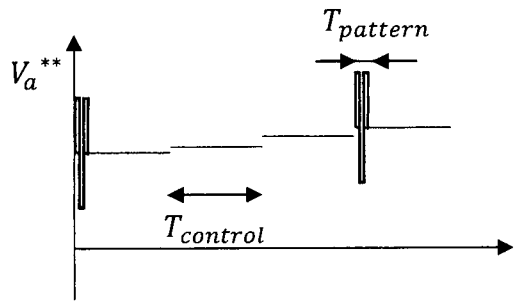


Fig. 17

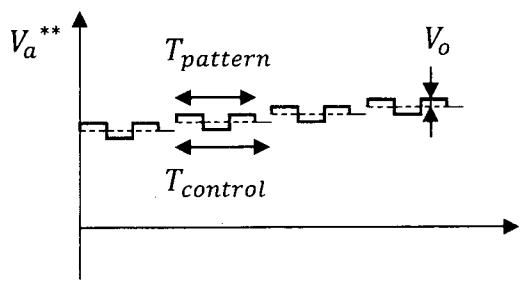


Fig. 18

INTERNATIONAL SEARCH REPORT

International application No
PCT/JP2020/047311

A. CLASSIFICATION OF SUBJECT MATTER
INV. H02P21/13 H02P21/18 H02P21/22 H02P21/32
ADD.

According to International Patent Classification (IPC) or to both national classification and IPC

B. FIELDS SEARCHED

Minimum documentation searched (classification system followed by classification symbols)
H02P

Documentation searched other than minimum documentation to the extent that such documents are included in the fields searched

Electronic data base consulted during the international search (name of data base and, where practicable, search terms used)
EPO-Internal, WPI Data

C. DOCUMENTS CONSIDERED TO BE RELEVANT

Category*	Citation of document, with indication, where appropriate, of the relevant passages	Relevant to claim No.
X	EP 2 515 431 A2 (HITACHI IND EQUIPMENT SYS [JP]) 24 October 2012 (2012-10-24)	1,7,9-12
Y	abstract	2-4,6,8
A	paragraphs [0005], [0029] - [0036]	5
	figures 1-17	
	claim 1	

A	WO 2009/024835 A1 (FREESCALE SEMICONDUCTOR INC [US]; BALAZOVIC PETER [CZ] ET AL.) 26 February 2009 (2009-02-26)	1-12
	abstract	
	page 7 - page 9	
	figures 1-3	

	-/--	

[X] Further documents are listed in the continuation of Box C.

[X] See patent family annex.

* Special categories of cited documents :

"A" document defining the general state of the art which is not considered to be of particular relevance

"E" earlier application or patent but published on or after the international filing date

"L" document which may throw doubts on priority claim(s) or which is cited to establish the publication date of another citation or other special reason (as specified)

"O" document referring to an oral disclosure, use, exhibition or other means

"P" document published prior to the international filing date but later than the priority date claimed

"T" later document published after the international filing date or priority date and not in conflict with the application but cited to understand the principle or theory underlying the invention

"X" document of particular relevance; the claimed invention cannot be considered novel or cannot be considered to involve an inventive step when the document is taken alone

"Y" document of particular relevance; the claimed invention cannot be considered to involve an inventive step when the document is combined with one or more other such documents, such combination being obvious to a person skilled in the art

"&" document member of the same patent family

Date of the actual completion of the international search	Date of mailing of the international search report
3 March 2021	12/03/2021

Name and mailing address of the ISA/	Authorized officer
European Patent Office, P.B. 5818 Patentlaan 2 NL - 2280 HV Rijswijk Tel. (+31-70) 340-2040, Fax: (+31-70) 340-3016	Vanata, Daniela

1

Form PCT/ISA/210 (second sheet) (April 2005)

INTERNATIONAL SEARCH REPORT

International application No
PCT/JP2020/047311

C(Continuation). DOCUMENTS CONSIDERED TO BE RELEVANT

Category*	Citation of document, with indication, where appropriate, of the relevant passages	Relevant to claim No.
Y	EP 1 401 093 A2 (HITACHI LTD [JP]) 24 March 2004 (2004-03-24) abstract paragraph [0041] - paragraph [0053] claim 1 figures 1-8 -----	2-4,6,8

1

INTERNATIONAL SEARCH REPORT

Information on patent family members

International application No
PCT/JP2020/047311

Patent document cited in search report	Publication date	Patent family member(s)	Publication date
EP 2515431 A2	24-10-2012	CN 102751936 A	24-10-2012
		EP 2515431 A2	24-10-2012
		JP 5401500 B2	29-01-2014
		JP 2012228058 A	15-11-2012
WO 2009024835 A1	26-02-2009	CN 101779371 A	14-07-2010
		EP 2191564 A1	02-06-2010
		WO 2009024835 A1	26-02-2009
EP 1401093 A2	24-03-2004	EP 1401093 A2	24-03-2004
		JP 3695436 B2	14-09-2005
		JP 2004112898 A	08-04-2004
		KR 20040025530 A	24-03-2004
		US 2004051495 A1	18-03-2004